Sorting within the Regulated Secretory Pathway Occurs in the *trans*-Golgi Network

Wayne S. Sossin, Joseph M. Fisher, and Richard H. Scheller

Department of Biological Sciences, Stanford University, Stanford, California 94305

Abstract. Bioactive peptides cleaved from the egg-laying hormone precursor in the bag cell neurons of *Aplysia* are sorted into distinct dense core vesicle classes (DCVs). Bag cell prohormone processing can be divided into two stages, an initial cleavage occurring in a late Golgi compartment, which is not blocked by monensin, and later cleavages that occur within DCVs and are blocked by monensin. Prohormone intermediates are sorted in the *trans*-Golgi network. The large soma-specific DCVs turn over, while the small DCVs are transported to processes for regulated release. Thus, protein trafficking differentially regulates the levels and localization of multiple biologically active peptides derived from a common prohormone.

SECRETED peptide hormones are used to mediate cell–cell interactions in eucaryotic organisms. Most of these peptide hormones are synthesized as components of larger precursors that are subsequently cleaved and modified to produce the bioactive molecules. Within the central nervous system, both the processing of neuropeptides and the packaging of peptide products into dense core vesicles (DCVs),[1] are important events in regulating intercellular communication (Loh et al., 1984; Sossin et al., 1989). The subsequent exocytosis of these DCVs in response to specific stimuli, such as the action potential–induced influx of calcium, defines the pathway of regulated secretion.

Many events specific to neuropeptide processing, such as cleavage at dibasic sequences, trimming of basic residues, and carboxy-terminal amidation, take place after the packaging of prohormones into DCVs (Gainer et al., 1977; Orci et al., 1987; Tooze et al., 1987*a*). However, recent evidence suggests that the initial endoproteolytic cleavage of some prohormones occurs earlier in the secretory pathway before or during the formation of DCVs (Davidson et al., 1988; Fisher et al., 1988).

The packaging of neuropeptides is associated with a sorting event that separates molecules destined for the regulated secretory pathway from lysosomal proteins, plasma membrane constituents, and constitutively secreted products. This sorting and packaging is thought to occur at the *trans*-most region of the Golgi apparatus, the *trans*-Golgi network (TGN; Griffiths and Simons, 1986; Tooze et al., 1987*b*; Orci et al., 1988). While the mechanism of this sorting is still unknown, proposals have been made both for an aggregation event whereby the condensation of neuropeptides excludes other proteins from the forming DCV (Kelly, 1985), and a receptor-mediated sorting event (Burgess and Kelly, 1987; Pfeffer and Rothman, 1987; Chung et al., 1989) analogous to lysosomal sorting where a specific signal (mannose-6-phosphate) targets proteins through a recycling receptor (Griffiths et al., 1988).

Sorting within the regulated secretory pathway has recently been demonstrated both in Somatomammotrophs (Fumagalli and Zanini, 1985; Hashimoto et al., 1987) and in the bag cell neurons of *Aplysia californica* (Fisher et al., 1988). In the bag cells, different products of the egg-laying hormone (ELH) precursor are localized to separate classes of DCVs. Peptides from the carboxy-terminal side of the ELH precursor are found in a class of small DCVs which are rapidly transported to the neuronal processes, while peptides from the amino-terminal side of the precursor are found both in a class of large DCVs that are restricted to the cell body and a distinct class of small DCVs which are transported to processes (Fig. 1). This sorting event has important physiological consequences as the different regions of the ELH prohormone contain peptides with unique biological activities (Kupfermann, 1967; Rothman et al., 1983*a*,*b*; Mayeri et al., 1985; Kauer et al., 1987; Brown and Mayeri, 1989).

In this paper, we investigate the cellular pathway of protein trafficking within the bag cells using EM autoradiography and the carboxylic acid ionophore monensin. The bag cells have two features that facilitate these studies; (*a*) the ELH prohormone is the major protein produced by the bag cells and accounts for up to 50% of the translated protein (Berry and Arch, 1981; Scheller et al., 1983); (*b*) an asymmetric distribution of amino acids across the prohormone (Fisher et al., 1988; Fig. 1) allows the selective labeling of the sorted

W. S. Sossin's present address is Center for Neurobiology and Behavior, Columbia University College of Physicians and Surgeons, 722 West 168th St., New York, NY 10032.

1. *Abbreviations used in this paper*: ASW, artificial sea water; DCV, dense core vesicles; ELH, egg-laying hormone; HD, half-distance; Ile, isoleucine; Phe, phenylalanine; TGN, *trans*-Golgi network.

carboxy or amino terminal–derived peptides. In this study, we use these properties to selectively follow the flow of neuropeptides derived from the ELH precursor through the secretory pathway. The results suggest possible mechanisms that underlie sorting within the regulated secretory pathway.

Materials and Methods

EM Autoradiography

250–750-g *Aplysia* were obtained from Sea Life Supply (Sand City, CA). Bag cell clusters were isolated and equilibrated in artificial sea water (ASW; 490 mM NaCl, 11 mM KCl, 19 mM $MgCl_2$, 30 mM $MgSO_4$, 11 mM $CaCl_2$, and 10 mM Tris, pH 7.6) at 14°C for 30 min. The clusters were then incubated in ASW and L-[4-5-^{3}H]isoleucine ([^{3}H]Ile) or L-[2, 3, 4, 5, 6-^{3}H]phenylalanine ([^{3}H]-Phe)(Amersham Corp., Arlington Heights, IL) (1 mCi/ml for a 30-min pulse; 4 mCi/ml for a 5-min pulse) for either 5 or 30 min and then chased with ASW plus 1 mM Phe, ASW plus 1 mM Ile, or isotonic L15 plus 1 mM Phe for the 12-h chase at 14°C. The chase was stopped by placing the clusters into a fixation solution consisting of 2% glutaraldehyde, 2% paraformaldehyde, 1% DMSO, 0.3 M sucrose in PBS (0.137 M NaCl, 25.5 mM KCl, 8 mM Na_2PO_4, 1.5 mM KH_2PO_4, pH 7.4). Occasionally, 1% acrolein was also included in the fixation solution. The tissue was fixed for 4–6 h at room temperature (occasionally overnight at 4°C). The clusters were rinsed with PBS, desheathed, and osmicated with 2% OsO_4 in PBS for 2 h followed by four washes in DDH_2O and an additional 2 h in 2% aqueous uranyl acetate. The clusters were then step-wise dehydrated to 100% ethanol followed by propylene oxide before infiltrating and embedding with Epon-Araldite. After polymerization, thin sections (80–100 nm) were cut on a microtome (Reichert Jung, Vienna, Austria) and collected on formvar-coated nickel grids. The grids were then lead stained, carbon coated, and covered with emulsion L4; Ilford Ltd., Basildon, Essex, England) using the loop technique (Caro and Van Tubergen, 1962; Caro, 1969; Williams, 1977). The emulsion was exposed in the dark at 4°C from 2 d to 1 mo depending on the experiment and then developed by incubating in Microdol X (Eastman Kodak Co., Rochester, NY; 3 min), stopped in 1% acetic acid, fixed with 30% sodium thiosulfate (3 min), and washed in DDH_2O. Grids were then visualized using a transmission electron microscope (410; Philips Electronic Instruments, Inc., Mahwah, NJ).

Quantitation of EM Autoradiography

Micrographs were photographed at 16,900× and then printed to give a final magnification of 45,000×. This size was chosen as the smallest magnification that small clear vesicles around the Golgi apparatus are clearly visible. Pictures were not taken at grid coordinates but rather over concentrations of grains. This was necessary due to the large size of the bag cells (50 μM in diameter) and the small area of the cells in which one could find grains. Therefore, all results are given in percentage of grains in each compartment rather than density of radioactivity in each compartment.

The micrographs were digitized (GP7 digitizer; Science Accessories Corp., Southport, CT) and analyzed using a computer-implemented maximum likelihood algorithm (Miller et al., 1985). An important parameter in this program is the approximate error due to the spread of radioactivity, which depends on the thickness of the section and the emulsion. We calculated all time points at half-distance (HD) values (Saltpeter and Bachmann, 1972) of 165, 190, and 230 nm. The calculations are fairly insensitive to this parameter, and the data in Table I are calculated with an HD of 190 nm, as this value matched our estimates for section and emulsion thickness. The largest variations observed at different HD values occur between the cytoplasm, ER, and small mature vesicles. All of these compartments have large areas and low densities and are situated in close proximity to each other, making it difficult to asign counts between these compartments. The largest change is seen at the Ile 30-min pulse plus 4-h chase time point, when, with an HD of 230 nm, the percentage of counts in small mature vesicles and cytoplasm are 34.3 and 21.3%, respectively, as opposed to 17.6 and 55.4% with an HD of 165 nm. All other changes were minor in comparison, and in the compartments important in these studies – small and large immature vesicles, clear vesicles, and Golgi apparatus – the results between calculations at three HD values differ by no more than 5% in any experiment.

There were nine compartments entered during digitization of the micrograph (ER, Golgi apparatus, Golgi-associated sacs [usually situated on the *cis* side of the Golgi apparatus], DCVs, immature DCVs, clear vesicles, mitochondria, lysosomes, and nucleus). All nonlabeled parts of the micrographs defaulted to cytoplasm. Mature and immature DCVs were then divided into small and large classes using a size cutoff (area = 49,000 nm^2, based on a diameter of 250 nm; Fisher et al., 1988) to make a total of 12 compartments. The areas of labeled (center of at least one grain within the vesicle) and unlabeled large vesicles were also calculated to determine if Phe-labeled small immature DCVs gradually increased in size to form large Phe-labeled immature DCVs. At the earliest time point that significant radioactivity is observed in large immature vesicles (Phe 5-min pulse plus 45-min chase), the average area of labeled large vesicles was actually larger than the average area of unlabeled large vesicles (1.2×) and exceeded the cutoff size by a large margin (average diameter = 490 nm). Immature vesicles were defined by either (*a*) membrane extensions (bulge or sac; see Fig. 2); (*b*) irregularities in shape; (*c*) extremely ruffled membranes; or (*d*) connection to a tubule or Golgi stack. It is important to note that the percentage of immature vesicles is probably an underestimate, as serial sections through bag cells often reveal sacs on vesicles or connections to tubules that are absent in other sections. For the Phe 30-min pulse plus 12-h chase experiment, the lysosome compartment was divided into mottled DCVs and clear lysosomes. For all experiments other than Phe 30-min pulse plus 12-h chase, the digitization was done blindly without knowledge of the time point or the label used in the experiment.

Most time points include data from more than one application of emulsion. Data was pooled from experiments as long as the average number of

Table I. Quantitation of EM Autoradiography

Pulse (min)	30	30	30	30	30
Chase (min)	0	30	120	240	30
Amino acid	Ile	Ile	Ile	Ile	Phe
ER	11.0 ± 1.1	3.8 ± 1.4	1.7 ± 1.4	<0.1 ± 1.4	3.3 ± 1.6
Golgi stacks	25.9 ± 0.8	15.3 ± 2.3	3.2 ± 1.2	5.3 ± 1.2	29.5 ± 1.1
Golgi vacuoles	6.4 ± 1.5	0.7 ± 0.6	1.6 ± 1.1	0.1 ± 0.7	8.7 ± 2.1
Clear vesicles	8.9 ± 1.8	23.7 ± 4.3	11.3 ± 0.9	4.5 ± 1.4	14.3 ± 1.2
Small immature DCV	11.0 ± 1.0	22.8 ± 2.7	34.3 ± 1.5	13.0 ± 1.7	20.3 ± 2.5
Large immature DCV	<0.1 ± 0.0	0.7 ± 0.4	3.1 ± 0.7	2.0 ± 0.9	1.5 ± 0.3
Small mature DCV	11.8 ± 2.2	15.3 ± 1.9	25.6 ± 2.3	19.5 ± 4.0	5.9 ± 1.0
Large mature DCV	1.7 ± 0.6	0.3 ± 0.2	2.6 ± 1.2	0.3 ± 0.3	0.4 ± 0.2
Lysosomes	<0.1 ± 0.3	<0.1 ± 0.2	<0.1 ± 0.2	<0.1 ± 0.5	<0.1 ± 0.1
Mottled DCV	ND	ND	ND	ND	ND
Mitochondria	2.1 ± 0.6	3.5 ± 0.9	2.8 ± 1.1	2.8 ± 1.5	<0.1 ± 0.1
Nucleus	<0.1 ± 0.0	<0.1 ± 0.0	0.1 ± 0.2	0.7 ± 0.4	<0.1 ± 0.3
Cytoplasm	20.8 ± 2.5	15.0 ± 3.2	13.5 ± 3.5	51.7 ± 4.6	16.0 ± 2.2
Grains (*n*)	663	745	533	631	1021
Micrographs (*n*)	35	88	60	47	63

Values are given in percentage of counts. Standard deviations are calculated from simulations as described in Materials and Methods.

grains per micrograph was within 20%. For the Phe 5-min pulse plus 1-h chase experiment, results are a weighted average of two different sets of data.

The standard deviations in Table I are the result of simulation experiments (Miller et al., 1985) to evaluate the error inherent in the quantitation. In these experiments, new grains for each micrograph were generated using the assumptions inherent in the algorithm (a poisson distribution of grains in a compartment and a gaussian error vector between the location of the radioactivity and the center of the simulated grain). The maximum likelihood calculation was then repeated for the simulated grains. Five simulations were done for each time point, and the standard deviation of these simulations is presented in Table I. In several cases, the original value was not within one standard deviation of the simulation average, although all values were within two standard deviations. This occurred mainly in the small mature and clear vesicle compartments and is probably caused by the inhomogeneity of these compartments. For example, the clear vesicle compartment contains transport vesicles from ER to Golgi apparatus, from one Golgi stack to another, and from Golgi apparatus to plasma membrane as well as parts of the TGN, primary lysosomes, and other compartments that cannot be differentiated by morphology. The simulation treats these as homogeneous compartments, while the grains may have been coming from a small subset of these compartments. Therefore, the simulations arrive at estimates different from the original computation. The small mature vesicles at early time points are usually found close to the Golgi apparatus and thus do not share the distribution of the majority of small mature vesicles, again causing differences between the simulation and the original experiment. Other errors, such as sampling bias and digitation errors, are not included in the standard deviations and probably add to the total error in the experiment. It is difficult to quantitate these errors and they are presumed to be minor contributions compared with the errors due to the quantitation procedure.

Simulations were also used to evaluate the possibility that the high percentage of grains in clear vesicles resulted from their proximity to both Golgi apparatus and small immature vesicles. At three time points (Phe 30-min pulse plus 30-min chase, Ile 30-min pulse plus 30-min chase, and Phe 5-min pulse plus 30-min chase), the counts in clear vesicles were assigned proportionally to Golgi apparatus and small immature vesicles, and a total of 10 simulations were carried out with these new densities. In these 10 simulations, the maximum value of counts ever seen over clear vesicles is 3%, and thus we conclude that the high values seen over this compartment at these time points is not due to their proximity to other compartments that contain radioactivity.

One source of concern is the relative incorporation and washout of [^{3}H]Ile and [^{3}H]Phe. As our results are mainly based on comparing the flow of the different regions of the prohormone, as opposed to comparing the absolute position at a time point, we do not feel that possible differences in incorporation and washout would affect our results. The relatively slow washout of accumulated [^{3}H]Phe probably accounts for the difference in absolute timing observed between the experiments with 5- and 30-min pulses of [^{3}H]Phe.

Acid Phosphatase

Bag cell clusters were isolated and fixed in 1% glutaraldehyde, 2% paraformaldehyde, 1% DMSO, 0.3 M sucrose in 0.1 M Na cacodylate buffer, pH 7.4, for 90 min at 4°C. The sheath was then dissected from the cluster, and the cluster was washed in 0.05 M Na Acetate, pH 5, and incubated in 0.1% cytidine monophosphate (Sigma Chemical Co., St. Louis, MO) or glycerophosphate (Sigma Chemical Co.) and 0.15% lead nitrate in 0.05 M Na acetate, pH 5, for 90 min at 37°C (Novikoff et al., 1971). Results were similar for both of the labels, and control preparations without substrate showed no lead precipitate. Clusters were washed with 0.1 M Na cacodylate, pH 7.4, osmicated in 2% OsO_4 in 0.05 M Na cacodylate, pH 7.4, for 1 h, and then dehydrated and embedded as described above. Thin sections (80–100 nm) were cut and stained with 2% uranyl acetate followed by lead nitrate before visualization on a transmission electron microscope (410; Philips Electronic Instruments, Inc.).

Monensin Experiments

Bag cell clusters or atrial gland pieces were incubated in 10 μM monensin (Sigma Chemical Co.) for 2 h in ASW with 1% ethanol at 14°C. Control experiments with ASW and 1% ethanol alone showed no effect on the bag cells. After the 2-h preincubation, clusters were labeled with tritiated amino acids as described above. All incubations and washes were done in the presence of 10 μM monensin and 1% EtOH or 1% EtOH alone. The clusters were then processed for EM immunohistochemistry (Fisher et al., 1988), autoradiography (described above), or SDS-urea gels (Newcomb et al., 1988).

In the monensin EM autoradiography experiment, quantitation was similar to that already described, but different compartments were used. The compartments measured in the monensin experiment were ER, vacuoles, vacuoles with densities, densities in vacuoles, dense core vesicles, mitochondria, lysosomes, nucleus, and cytoplasm. A separate compartment, vacuolar membranes, was calculated in the entry algorithm. As the vacuoles curve through the thickness of the section, a 50-nm distance was used to define the limit of the membrane in these calculations. Also, for quantitating monensin experiments, micrographs were taken at 12,000× magnified to 32,000×.

Time Course of Processing

Clusters were labeled as described (Newcomb et al., 1988). The gels were quantitated by densitometry of the x-ray film.

Results

Time Course of Processing of the ELH Prohormone

Sorting of the carboxy- and amino-terminal regions of the

30	30	30	5	5	5
120	240	720	30	45	60
Phe	Phe	Phe	Phe	Phe	Phe
0.6 ± 0.9	5.6 ± 0.8	0.4 ± 0.7	3.2 ± 1.8	0.4 ± 1.1	<0.1 ± 0.8
0.3 ± 0.3	2.3 ± 0.4	2.0 ± 0.5	12.0 ± 3.4	2.8 ± 0.7	<0.1 ± 0.4
<0.1 ± 0.3	<0.1 ± 0.1	<0.1 ± 0.4	<0.1 ± 0.8	<0.1 ± 0.0	<0.1 ± 0.3
5.6 ± 3.2	12.2 ± 2.2	1.8 ± 0.7	24.4 ± 4.2	15.0 ± 1.8	10.9 ± 2.6
11.5 ± 1.3	7.5 ± 1.2	4.2 ± 0.8	33.7 ± 4.1	18.8 ± 1.1	12.5 ± 2.1
48.2 ± 1.1	27.6 ± 1.0	4.9 ± 0.3	7.2 ± 1.6	36.1 ± 1.7	34.3 ± 5.2
11.5 ± 1.5	9.1 ± 1.6	16.2 ± 2.2	13.8 ± 2.3	3.8 ± 0.3	7.9 ± 3.0
15.7 ± 1.6	23.4 ± 1.8	18.3 ± 0.5	5.4 ± 2.1	12.5 ± 0.5	24.2 ± 9.9
0.2 ± 0.3	<0.1 ± 0.2	3.0 ± 0.5	<0.1 ± 0.5	0.6 ± 0.6	0.4 ± 0.3
ND	ND	37.9 ± 1.0	ND	ND	ND
<0.1 ± 0.4	<0.1 ± 0.2	<0.1 ± 0.1	0.2 ± 0.5	1.1 ± 0.2	0.3 ± 0.4
0.8 ± 0.3	0.3 ± 0.3	<0.1 ± 0.1	<0.1 ± 0.0	<0.1 ± 0.0	<0.1 ± 0.0
5.6 ± 1.8	11.7 ± 1.6	11.0 ± 3.0	<0.1 ± 1.0	7.4 ± 1.6	8.7 ± 6.0
827	572	1230	276	700	793
108	87	104	70	63	101

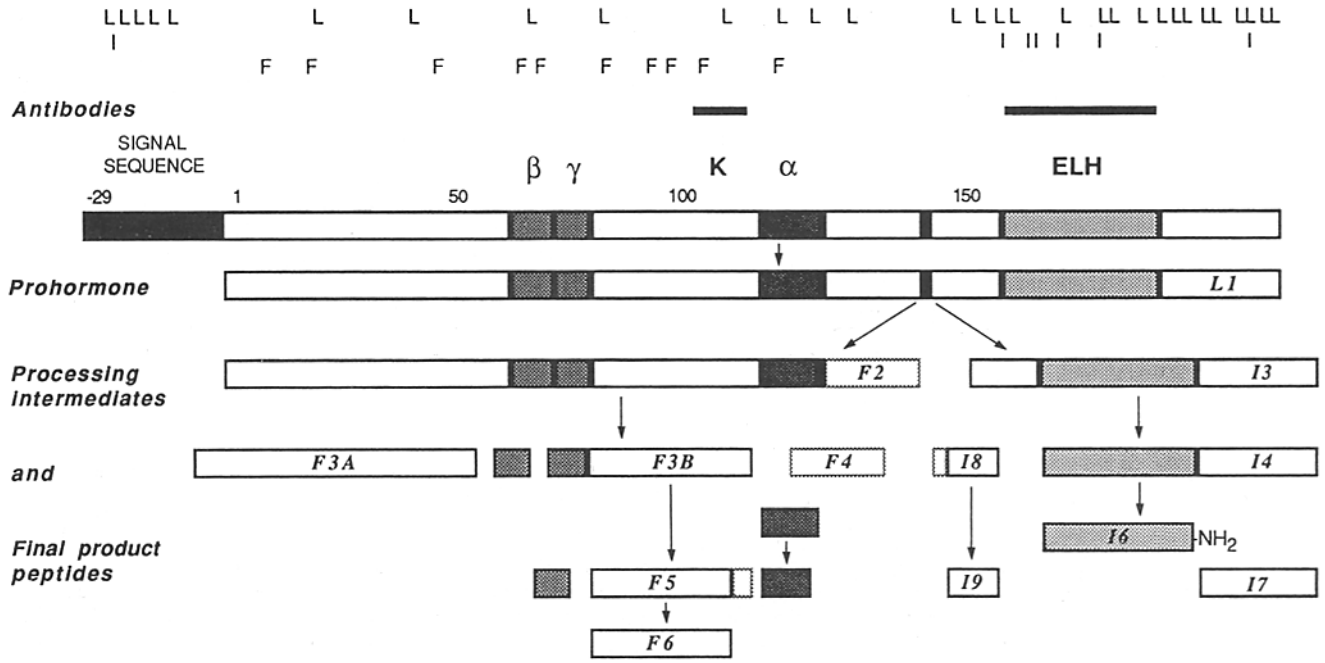

Figure 1. Proteolytic processing of the ELH prohormone. A schematic of the 242-amino acid ELH prohormone is shown including a 29-amino acid signal sequence (*horizontal black bars*). Four biologically active bag cell peptides, the α, β, and γ bag cell peptides as well as ELH, are shaded. Vertical bars are sequences of basic residues used as proteolytic processing sites. The first cleavage of the prohormone occurs at a tetrabasic sequence Arg-Arg-Lys-Arg, and the pathway then proceeds as shown, leading to the final set of product peptides shown (Newcomb et al., 1988). The peptides amino terminal to the first cleavage are packaged into one set of vesicles, and the peptides carboxy terminal to this cleavage are packaged in a distinct vesicle class. Above the schematic are the positions of the peptides used to raise antisera used in immunohistochemical experiments (Fisher et al., 1988). The top of the figure shows the distribution of the amino acids—leucine (*L*), isoleucine (*I*), and phenylalanine (*F*)—within the prophormone's sequence.

ELH precursor must occur after the initial cleavage of the prohormone. To determine the intracellular site of various cleavages, we have correlated the extent of prohormone endoproteolytic cleavage with the location of the molecule within the secretory pathway. Bag cell clusters were labeled with [^{3}H]Ile to label the carboxy-terminal, ELH-containing side of the prohormone or [^{3}H]Phe to label the amino-terminal, bag cell peptide-containing side of the prohormone. Acid acetone extracts were then fractionated on SDS-urea polyacrylamide gels (Fig. 2, *A* and *B*). After a 30-min pulse of radioactivity, no cleavage of the prohormone is observed ($n = 4$). The initial cleavage occurs after a 30-min pulse and a 30-min chase, although the percentage of cleavage at this time point is somewhat variable (68 ± 23% of prohormone cleaved; $n = 5$, three experiments with [^{3}H]Ile and two experiments with [^{3}H]Phe; no significant difference between [^{3}H]Phe and [^{3}H]Ile, $p > 0.5$). In experiments using 5-min pulses of [^{3}H]Phe, processing was mostly complete (80%, $n = 1$) after a 30-min chase and totally complete after a 1-h chase (data not shown). Consistent with previous results (Newcomb et al., 1988), further cleavage of the initial amino-terminal intermediate (F2; Fig. 2 *A*) occurs more slowly than that of the initial carboxy-terminal intermediate (I3; Fig. 2 *B*).

Treatment with Monensin Separates Processing of the Prohormone into Two Stages

Monensin is an ionophore that blocks the proteolytic cleavage of a number of neuropeptide prohormones and causes them to accumulate in Golgi-related compartments (Crine and Dufour, 1982; Orci et al., 1984). Presumably, the cleavage is inhibited either by blocking transport of the hormone to the site of cleavage or by disrupting necessary ionic gradients. In contrast to other systems, initial cleavage of the ELH prohormone still occurs after a monensin block; however, all subsequent cleavages are inhibited, and the two initial processing intermediates accumulate in monensin-treated cells (Fig. 2 *C*) (Yates and Berry, 1984). This is not a peculiar effect of monensin in *Aplysia* tissue, as all cleavages of the atrial gland prohormone are blocked after incubation with monensin (Fig. 2 *C*). Therefore monensin divides ELH processing into two distinct steps: the initial cleavage, which occurs before the monensin block, and all subsequent cleavages.

To identify the site of the monensin block, we examined monensin-treated bag cells in the electron microscope. As in other systems, monensin causes a specific enlargement of Golgi-related compartments while leaving other cellular compartments such as the nucleus, ER, mitochondria, lysosomes, and mature DCVs relatively unchanged (Tartakoff, 1983). In the bag cells, some of these vacuoles contain dense core material, and these can be divided into two general types: (*a*) vacuoles with densities that are homogeneous in appearance (80%) and (*b*) vacuoles that contain two different types of densities (20%; Fig. 3 *A*). Examination of the densities with immunoelectron microscopy reveal that homogeneous dense cores contain intermixed carboxy-terminal (ELH) and amino-terminal (peptide K) immunoreactivity, but, as illustrated in Fig. 3 *B*, when two separate densities

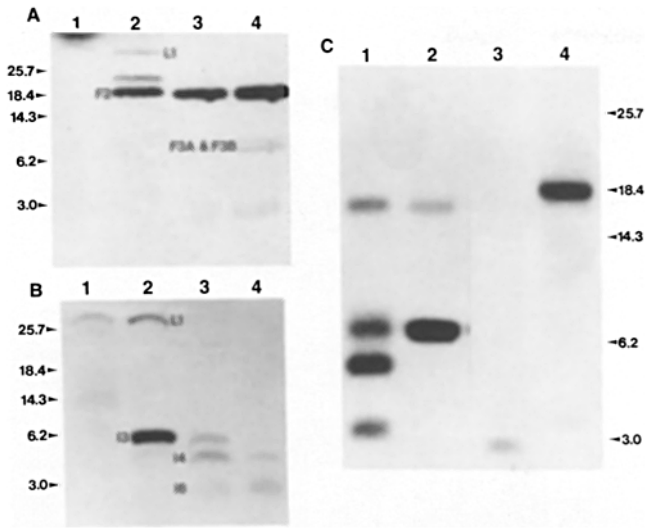

Figure 2. Time course of processing in normal and monensin-treated cells. Bag cell clusters were pulsed for 30 min with (*A*) [^{3}H]Phe or (*B*) [^{3}H]Ile and then chased for 0, 30, 120, or 240 min (lanes *1–4*). The clusters were then extracted with acid acetone and fractionated on SDS-urea gels. (Newcomb et al., 1988). The bands are marked according to the nomenclature outlined in Fig. 1 (Newcomb et al., 1988). The initial cleavage is occurring at the 30-min chase and is complete after 2 h. (*C*) After pretreatment for 2 h with 10 μM monensin plus 1% EtOH (lanes *2* and *4*) or ASW plus 1% EtOH (lanes *1* and *3*), bag cell clusters (lanes *1* and *2*) or atrial gland fragments (1 mm × 1 mm; lanes *3* and *4*) were pulsed for 2 h with [^{3}H]leucine and chased for 4 h (bag cells) or 20 h (atrial glands) before acid acetone extraction. Under these conditions, the initial cleavage of the bag cell prohormone is completed in monensin, but all further cleavages of the intermediates are blocked (lane 2). In contrast, the atrial gland precursor accumulates in monensin-treated cells (lane *4*). Other bag cell clusters labeled with [^{3}H]leucine were assessed by HPLC analysis (Newcomb and Scheller, 1987), and all radioactivity was found in the first intermediates, demonstrating more conclusively that no further cleavages of the F2 or I3 intermediate occur in the monensin experiment (data not shown).

are observed the immunoreactivity of the different dense cores is segregated. To demonstrate that these densities actually represent the site of blockage, the monensin-treated bag cells were pulse chased with either [^{3}H]Leu, [^{3}H]Phe, or [^{3}H]Ile and processed for EM autoradiography. As evident in Fig. 3 *C*, the radioactivity is largely centered over the densities in vacuoles.

Quantitation of the [^{3}H]Phe and [^{3}H]Ile experiments reveal that over half of the grains are contained in dense cores found within the vacuoles (57.2% for [^{3}H]Ile [203 grains counted in 11 micrographs) and 53.5% for [^{3}H]Phe [266 grains counted in 10 micrographs]). Few counts were seen over granules (6.6% for [^{3}H]Ile and <0.1% for [^{3}H]Phe), demonstrating that the formation of mature granules is inhibited in monensin-treated cells. Other concentrations of grains were seen over the vacuolar membranes (7.7% for [^{3}H]Ile and 27.4% for [^{3}H]Phe) and cytoplasm (22.8% for [^{3}H]Ile and 17.2% for [^{3}H]Phe).

Monensin blocks transport at various sites in different systems but almost always blocks transport somewhere within the Golgi apparatus (Griffiths et al., 1983; Johnson and Schlessinger, 1980; Orci et al., 1984). Osmium, a specific marker for the *cis*-Golgi compartment (Friend and Murray, 1965), labels a subset of vacuoles but does not label vacuoles that contain densities (data not shown), suggesting the monensin block is beyond this point in the secretory pathway. The presence of sorted densities suggests that segregation occurs at this stage of prohormone processing and that the intermediates may have intrinsic abilities to aggregate selectively. These results must be interpreted cautiously as the disruption of ionic and pH gradients in monensin-treated cells may cause perturbations in the sorting process.

EM Autoradiography Demonstrates Sorting in the Bag Cells

In pulse–chase studies using either [^{3}H]Ile (carboxy-terminal) or [^{3}H]Phe (amino-terminal), counts flow through the secretory pathway from ER to Golgi apparatus to granules (Table I). After a 30-min pulse with [^{3}H]Ile, a large number of grains are seen over the Golgi apparatus (Fig. 4 *A* and Table I). Since at this time point no processing has occurred (Fig. 2 *B*), one can conclude that cleavage does not occur early in the Golgi apparatus. Both amino and carboxy terminal–associated radioactivity are transported through the Golgi stacks and enter small immature DCVs (defined by membrane extensions, connection to tubules, or nonspherical morphology) and clear vesicles after a 30-min pulse and 30-min chase (Fig. 4 *B*, Fig. 5, and Table I). This is the time point correlated with the initial cleavage of the prohormone (Fig. 2, *A* and *B*).

After a 30-min pulse and 2-h chase with [^{3}H]Phe, grains are found predominantly over large immature DCVs (Fig. 4 *C*, Fig. 5, and Table I), while grains are found predominantly over small immature DCVs at this time point when [^{3}H]Ile is used (Fig. 4 *D*, Fig. 5, and Table I). Therefore, we can conclude that after a 30-min pulse and 2-h chase, the two regions of the ELH prohormone have been sorted into distinct compartments. The EM autoradiographic results are a strong independent confirmation of immunohistochemical studies demonstrating that large DCVs contain more immunoreactivity from amino terminal–derived (Phe) peptides, while the majority of small DCVs contain more immunoreactivity from carboxy terminal–derived (Ile) peptides (Fisher et al., 1988; Kreiner et al., 1989).

To look more closely at the movement of the amino-terminal intermediate from small to large immature vesicles, a number of experiments were done using 5-min pulses of [^{3}H]Phe (Table I). The movement from small to large DCVs occurs quickly (largely between 30 and 45 min of chase), and a large percentage of counts are also seen in clear vesicles at these time points. The vectorial flow of the amino-terminal portion of the precursor appears to be from Golgi apparatus to clear vesicles and small immature DCVs then to large immature DCVs.

The flow of the amino-terminal intermediate from small to large immature vesicles could arise by (*a*) distinct amino-terminal specific small vesicles increasing in size or (*b*) movement of the amino-terminal intermediate from small immature vesicles containing carboxy-terminal intermediates to a distinct class of large immature vesicles. We favor the second possibility due to the fact that we do not see a gradual increase in the size of Phe-labeled immature vesicles

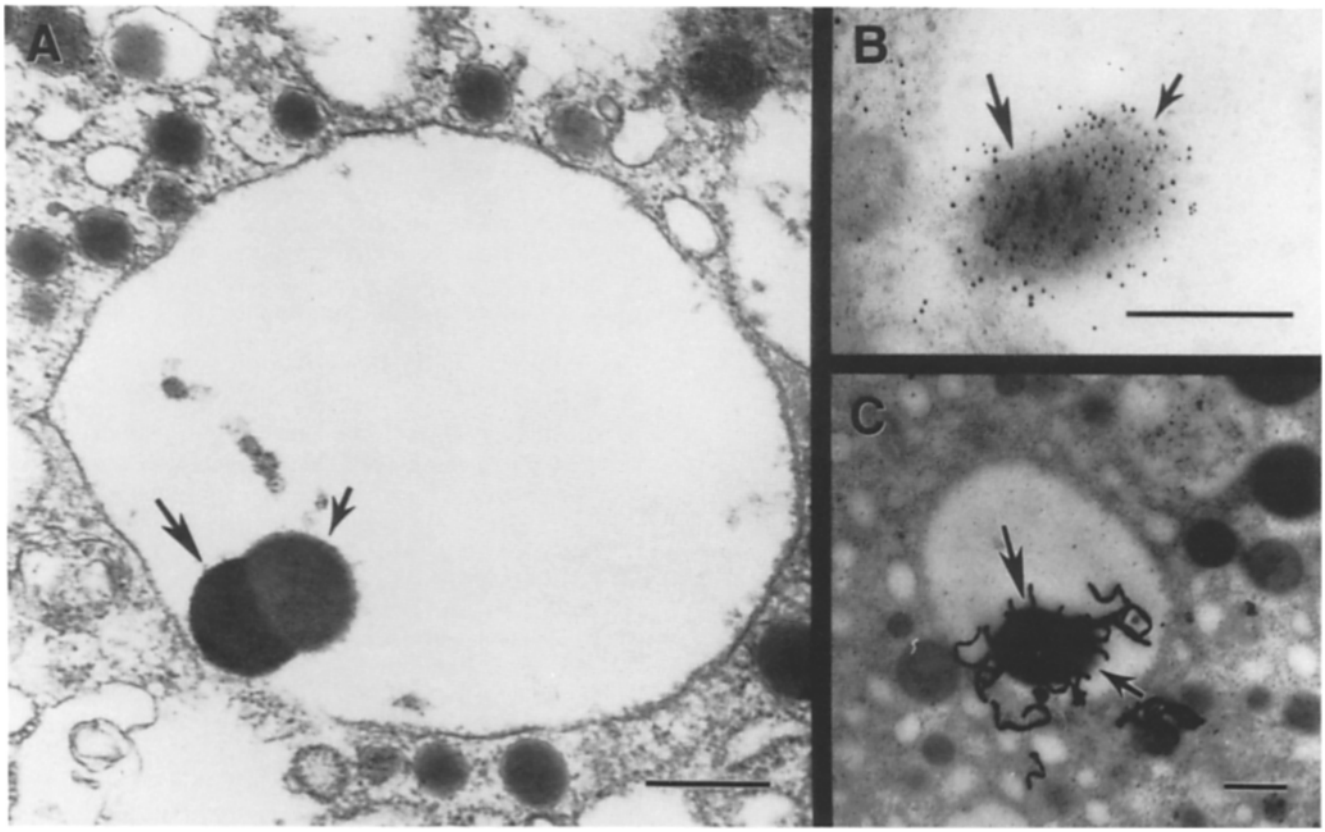

Figure 3. Intermediates accumulate in sorted densities in monensin-treated bag cells. (*A*) Monensin induces the formation of vacuoles in the bag cell soma, some of which contain dense cores. The small and large arrows identify two dense cores within a single vacuole that appear to be of different composition. About 10–20% of the densities in vacuoles had this appearance. (*B*) Immunoelectron microscopic analysis of monensin-treated bag cells. Bag cell sections were labeled with a rabbit anti-peptide K and a rat anti-ELH primary antibody followed by a 5-nm colloidal gold anti-rabbit and 10-nm colloidal gold anti-rat secondary antibodies. Immunoreactivity within the dense cores is segregated; the small arrow points to peptide K immunoreactivity, and the large arrow points to ELH immunoreactivity. (*C*) EM autoradiography of monensin-treated bag cells (2-d exposure). A bag cell cluster was preincubated for 2 h with monensin, labeled for 2 h with [^{3}H]leucine, and chased for 4 h. Grains are concentrated over the density in the vacuole (*arrow*), while mature granules outside of the vacuole are unlabeled. Bars, 400 nm.

(see Materials and Methods) but do observe an abrupt change from small to large Phe-labeled vesicles. Furthermore, small immature vesicles containing amino-terminal peptides that are contiguous with the Golgi apparatus are not observed, although carboxy-terminal peptide immunoreactive small immature vesicles are detected (Fisher et al., 1988).

The Small and Large Immature DCVs Are Part of the TGN

It is possible that features of immature vesicles may result from their association with the TGN. A standard marker for the TGN is acid phosphatase (Griffiths and Simons, 1986), and, as illustrated in Fig. 6, *A–C*, both small and large immature vesicle membranes are ringed by the lead phosphate reaction product. Immature vesicles have also been shown to contain acid phosphatase in a number of other systems (Smith and Farquhar, 1966; Novikoff et al., 1971; Hand and Oliver, 1977). Fig. 6, *A–C*, shows a series of micrographs from a set of serial sections; the structure marked by the small arrow actually attaches to the proximal large immature vesicle (Fig. 6 *A*) and in the next section attaches to a small immature vesicle (Fig. 6 *B*). Many other attachments between acid phosphatase–containing vesicles are seen in serial sections, suggesting that the immature vesicles are to some extent still connected to the tubular portion of the TGN. Mature small and large vesicles, as well as ER and other Golgi stacks, do not stain with acid phosphatase, while lysosomes stain intensely.

Double label experiments which combine EM autoradiography with acid phosphatase treatment formally demonstrate that the immature DCVs contain acid phosphatase activity (Fig. 6 *D*) and are therefore part of the TGN. Interestingly, one of the large vesicles in this micrograph contains only patches of acid phosphatase reaction product. This is a common occurrence and suggests that the acid phosphatase is removed in patches from immature vesicles, as opposed to gradually fading in intensity.

Acid phosphatase is an enzyme destined for transport to endosomes and lysosomes. The appearance of acid phosphatase reaction product in patches suggests that lysosomal proteins are removed, not only from clear regions of the TGN,

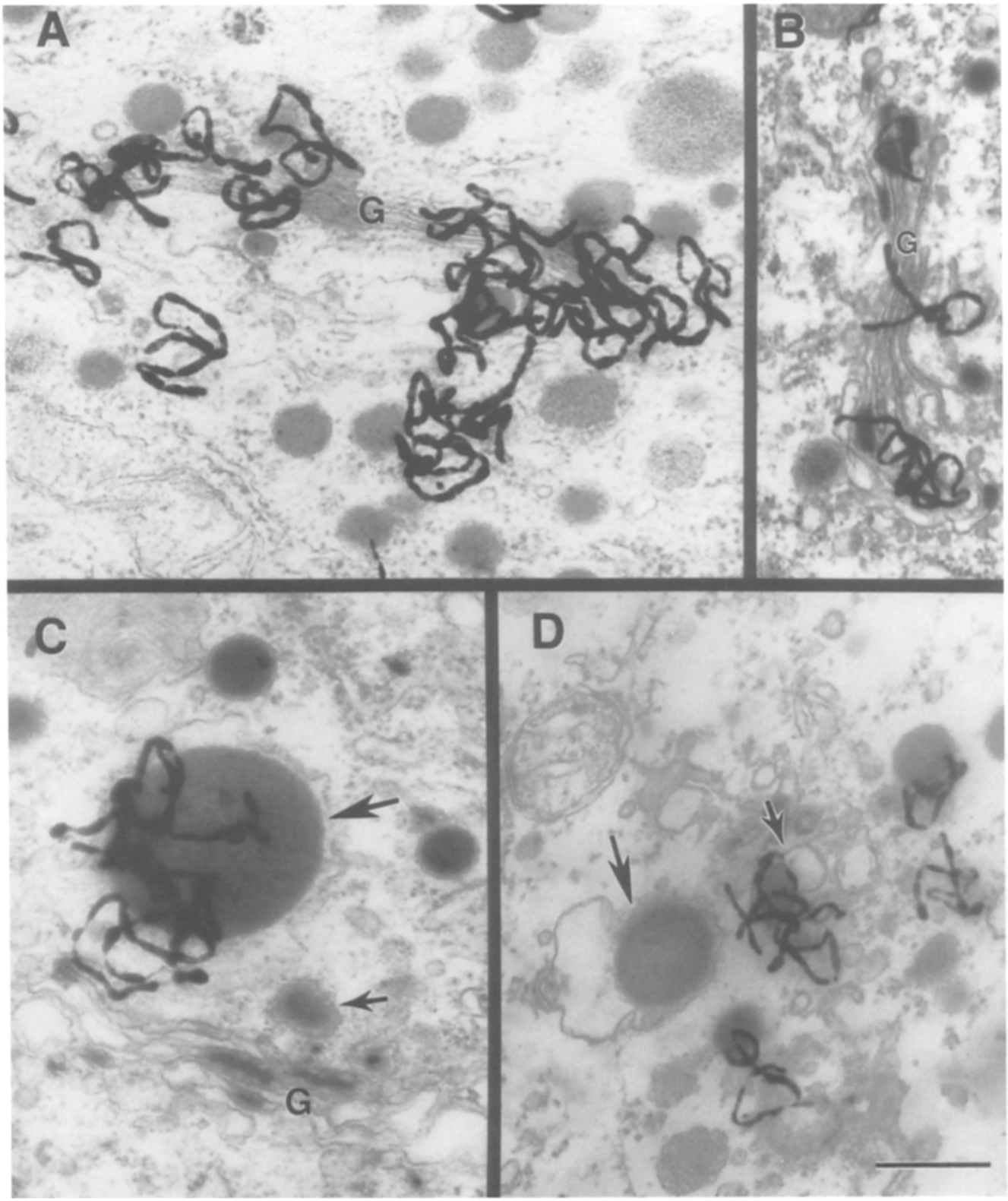

Figure 4. EM autoradiography demonstrates sorting in the bag cells. Thin sections of pulse-labeled bag cells processed for EM autoradiography. (*A*) 30-min pulse with [^{3}H]Ile. Grains are concentrated over the Golgi apparatus (4-d exposure). (*B*) 30-min pulse with [^{3}H]Ile and 30-min chase. Grains are concentrated over dense cores connected to Golgi apparatus and small immature vesicles (4-d exposure). (*C*) 30-min pulse with [^{3}H]Phe and 2-h chase. Grains are concentrated over large immature vesicles (*large arrow*) but not small immature vesicles (*small arrow*) (2-d exposure). (*D*) 30-min pulse with [^{3}H]Ile and 2-h chase. Grains are concentrated over immature small vesicles (*small arrow*) but not over immature large vesicles (*arrow*). Note the membrane extensions on these immature vesicles (4-d exposure). *G*, Golgi apparatus. Bar, 350 nm.

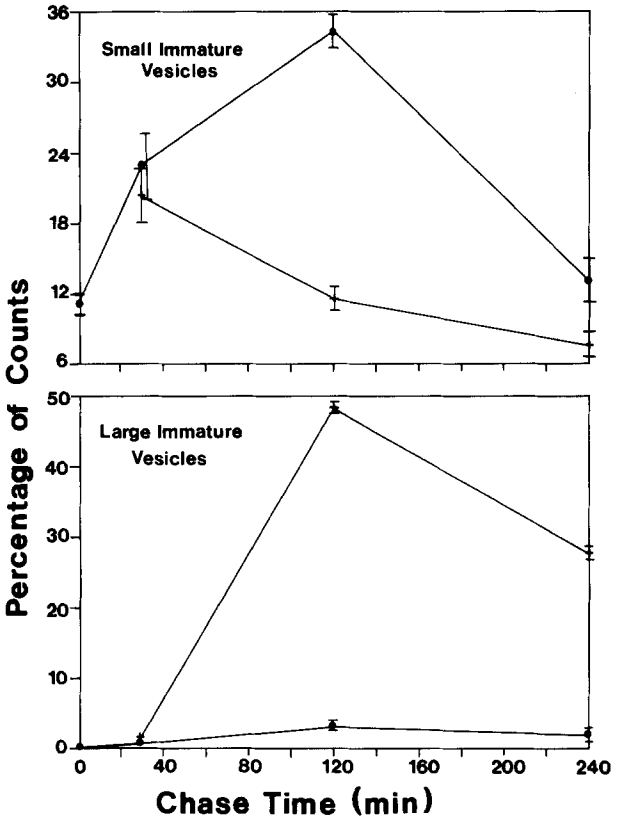

Figure 5. Sorting occurs within immature vesicles. The percentage of grains as calculated by the maximum likelihood method—(*A*) small immature vesicles and (*B*) large immature vesicles—is plotted as a function of the chase period for Phe (+) and Ile (•). The calculations for standard deviations are given in the methods. While after a 30-min chase there is little difference between the amino- (Phe) and carboxy-terminal (Ile) sides of the prohormone, after 2 h the two are in different compartments, suggesting that sorting occurs between those two times.

but also from membranes of immature vesicles. Immature vesicles often contain patches of clathrin, although the function of this clathrin is unclear. This clathrin has been proposed to be involved in the budding of regulated secretory vesicles (Orci et al., 1984, 1987) or recycling of protein from immature vesicles to the Golgi apparatus (Tooze and Tooze, 1986). Lysosomal enzymes are most probably removed via clathrin-coated vesicles from the TGN (Campbell and Rome, 1983; Griffiths and Simons, 1986; von Figura and Hasilik, 1986), suggesting that the function of clathrin patches on immature vesicles may be to facilitate sorting of lysosomal proteins.

The above results suggest that sorting occurs as the amino-terminal intermediate moves from small immature vesicles and clear vesicles to large immature vesicles, all of which are defined by acid phosphatase cytochemistry as part of the TGN. Furthermore, we have demonstrated the site of prohormone cleavage to be the clear vesicles, small immature vesicles, or Golgi stacks. Yet, at a time when the prohormone is intact (30-min pulse; Fig. 2 *B*), counts are located within the Golgi stacks (Fig. 3 *A*), suggesting that the cleavage of the prohormone must occur after this point, either in a late Golgi stack or, more likely, the TGN.

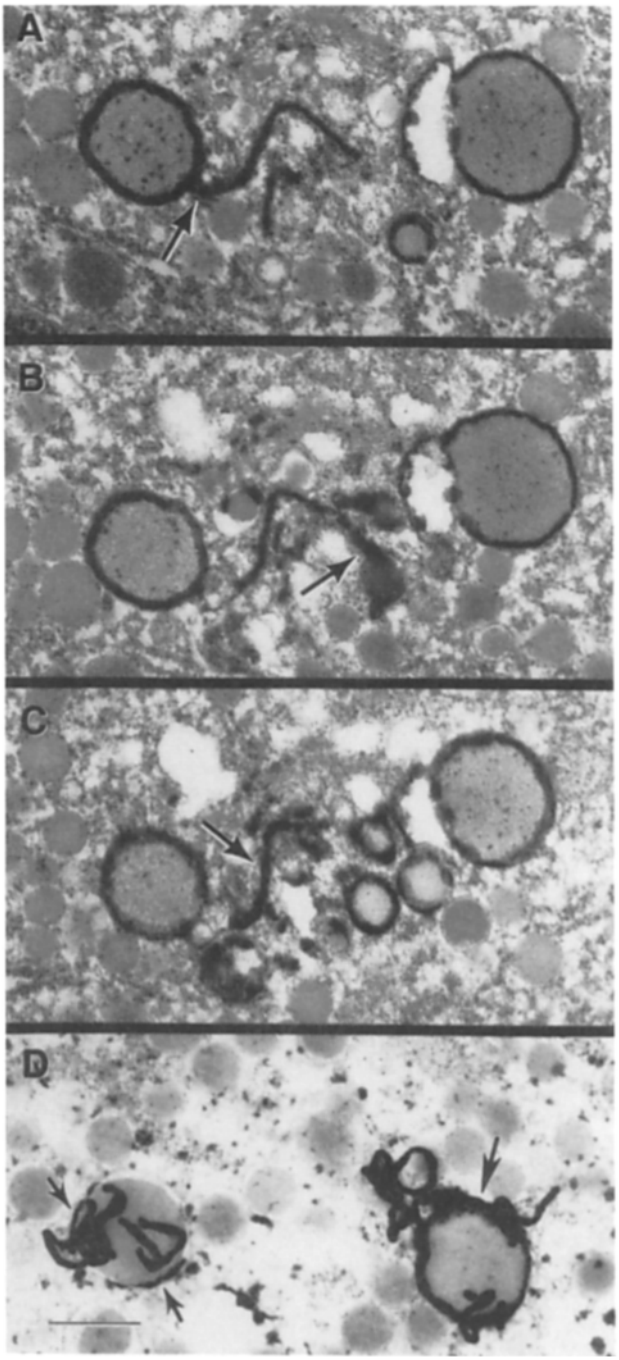

Figure 6. Immature vesicles are part of the TGN. (*A*) A bag cell treated to visualize acid phosphatase enzymatic activity reveals a network of tubules, small and large immature vesicles which comprise the TGN. The large arrow points to a tubule-like structure interconnected to a large immature vesicle. (*B*) In the next section, the large arrow points to the same tubule, which now appears interconnected to a small immature vesicle. (*C*) The large arrow, again, indicates the tubule-like structure. In this section, additional vesicles rimmed by acid phosphatase reaction product are apparent. (*D*) A bag cell cluster was pulsed for 30 min with [^{3}H]Phe and chased for 2 h. Before processing the cluster for EM autoradiography, the cluster was processed for acid phosphatase histochemistry. Arrows point to large immature vesicles that are both acid phosphatase positive and contain grains. The vesicle on the left has patches of membrane (*arrows*) with and without acid phosphatase reaction product, suggesting that lysosomal sorting has begun to occur. Exposure was for 1 wk. Bar, 350 nm.

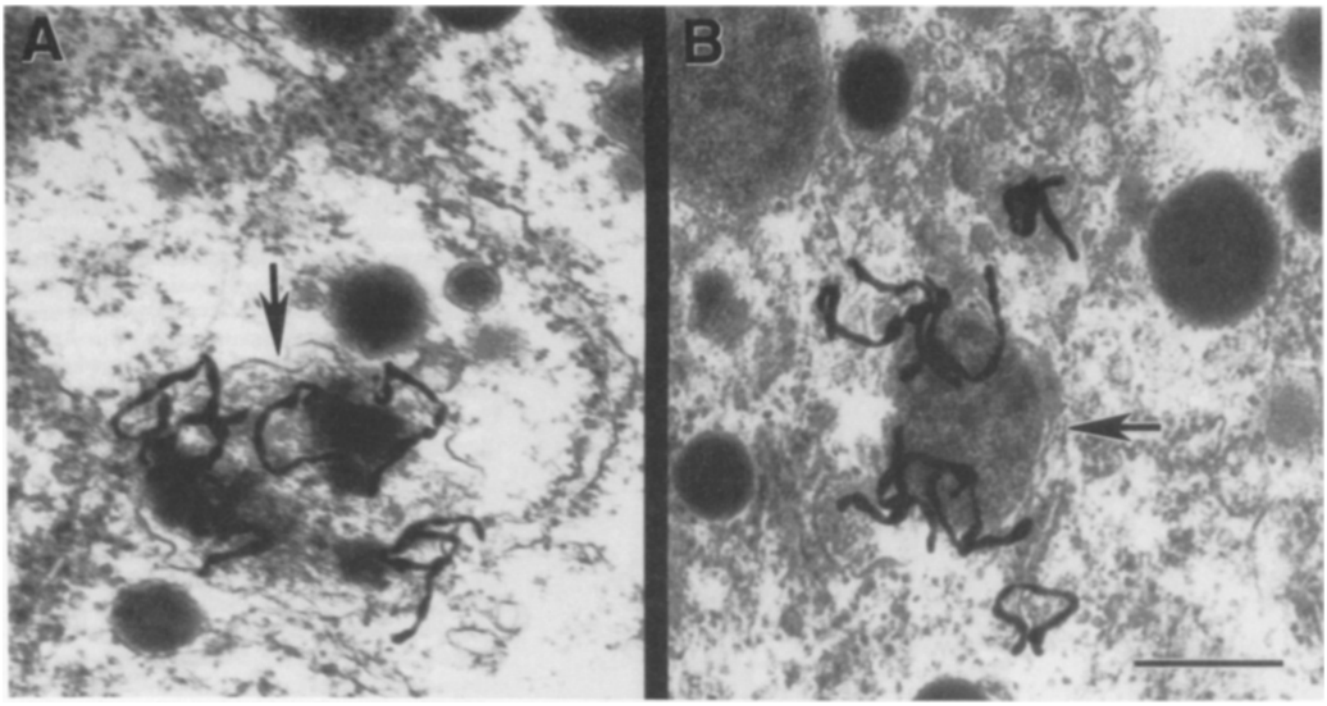

Figure 7. Large vesicles turnover after a 12-h chase. Bag cell clusters were pulsed for 30 min with [^{3}H]Phe and chased for 12 h. (*A* and *B*) Arrows point to examples of vesicles with heterogeneous cores (mottled vesicles). Approximately 40% of the counts appear in these compartments (Table I) at this time point. Exposure was for 3 wk. Bar, 350 nm.

Fate of the Large DCVs

Quantitative HPLC studies indicate that the carboxy-terminal (Ile) final product peptides are present at three- to eightfold higher steady-state levels than the amino-terminal (Phe) final peptides (Fig. 1; Fisher et al., 1988). The large DCVs are not transported to the processes (Kreiner et al., 1986) and quantitative immunoelectron microscopy studies suggest that the different levels of peptides could be due to the selective degradation or release of these large vesicles (Fisher et al., 1988). To examine this question we chased [^{3}H]Phe-labeled bag cell clusters for longer times to observe the eventual fate of the large DCVs. After 12 h of chase, many grains are observed in vesicles with heterogeneous cores that we refer to as mottled DCVs (Table I). The appearance of the core is quite variable, ranging from vesicles that are mostly clear but contained patches of dense material (Fig.7 *A*) to dense DCVs with nonhomogeneous patches (Fig. 7 *B*). Loss of the homogeneous dense core suggests the peptides are being degraded. Few grains are observed over large membranous lysosomes or multivesicular bodies. Other interesting results from this time point include the movement of grains from immature to mature large vesicles and an increase in the number of grains in small mature vesicles (Table I). Coupled with the lack of constitutive release of large vesicle contents (Fisher, J., unpublished data), these results suggest that the asymmetry in peptide steady-state levels is generated through a degradative pathway.

Discussion

A Model for Sorting within the Regulated Secretory Pathway

Our results suggest a model for sorting within the regulated secretory pathway (Fig. 8). Correlating a biochemical assay of processing with EM autoradiography predicts cleavage of the ELH prohormone in a late Golgi compartment. Further support for this model comes from subcellular fractionation studies of bag cells, where the initial cleavage is shown to occur in a light fraction enriched in mannosidase II activity (a Golgi marker) and well separated from the DCVs (Sweet, A., J. M. Fisher, W. S. Sossin, R. Newcomb, and R. H. Scheller, manuscript submitted for publication). The initial cleavage is not blocked by monensin, which does block the formation of mature granules. The protease that cleaves the tetrabasic site may be a TGN resident protein whose activity triggers the condensation and sorting of the processing intermediates in this compartment. Alternatively, processing enzymes with different pH activation profiles or different affinities for the various cleavage sites may explain the distinct subcellular sites of endoproteolytic cleavage in the bag cells. Multiple enzymes with different pH profiles have been proposed to differentiate between the two cleavages of the insulin precursor (Davidson et al., 1988).

After the initial cleavage event, the ELH-containing carboxy-terminal intermediate condenses in one region of the TGN (small immature vesicles) and the amino-terminal bag cell peptide–containing intermediate condenses in another region of the TGN (large immature vesicles). This model is consistent with immunocytochemical studies (Fisher et al., 1988) that demonstrate that small immature vesicles connected to the TGN contain largely carboxy-terminal immunoreactivity. These regions of the TGN may be connected by tubules, or transport between them may occur through vesicles.

How are these intermediates segregated before formation of a dense core? After a 30-min chase both amino and carboxy terminal–associated grains are found over small imma-

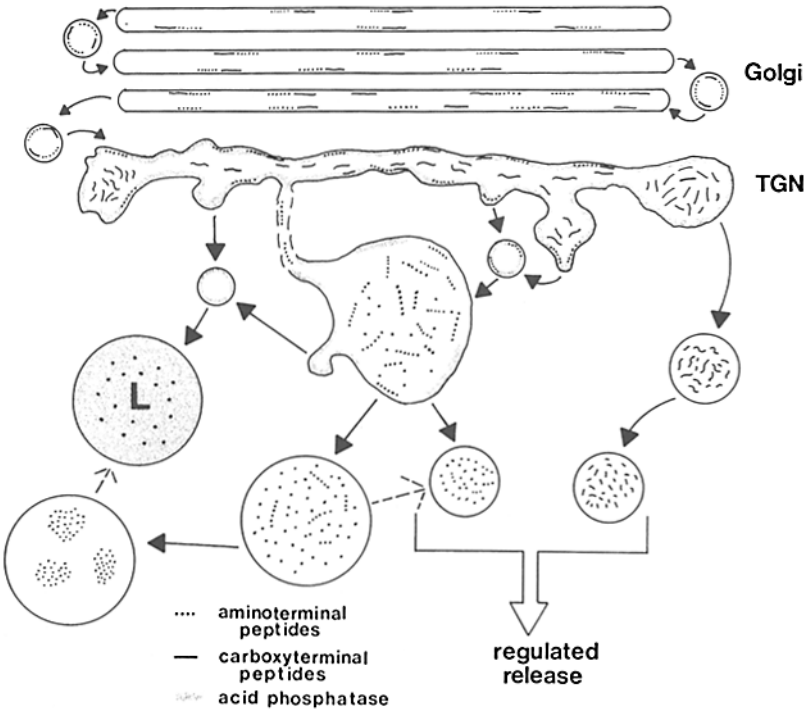

Figure 8. A model for sorting in the bag cells. A schematic diagram for prohormone processing and sorting in the bag cells is described fully in Discussion. A solid line represents the carboxy-terminal intermediate; a dotted line represents the amino-terminal intermediate; a dotted line attached to a solid line represents the ELH prohormone; smaller lines represent the carboxy-terminal final product peptides; and dots represent the amino-terminal final product peptides. L indicates an organelle of degradative function (endosome or lysosome). Direct connection between the part of the TGN containing large immature vesicles and small immature vesicles is putative and this is represented by a dotted line. Shading represents acid phosphatase–positive membranes. The small amino- and carboxy-terminal vesicles will be transported to processes for regulated release, where they are present at a carboxy-to-amino terminal ratio of 5:1 (Fisher et al., 1988).

ture vesicles and clear vesicles. Although the compartment of clear vesicles is obviously heterogeneous, the location and the time course of counts moving into these vesicles is most consistent with their arising from sections through the TGN. The lack of grains located over clear vesicles in other EM autoradiographic studies of neuropeptide transport (Saltpeter and Farquhar, 1981) may be due to an earlier peptide condensation event in that system. Amino terminal–associated radioactivity then decreases in clear vesicles and small immature granules and increases in large immature granules. It is the selective movement of the amino-terminal intermediate to large immature granules and/or the selective retention of the carboxy-terminal intermediate in small immature granules that underlies sorting within the regulated pathway. These results suggest a flow of the amino-terminal intermediate through the TGN from an early region that contains small immature vesicles to a later region that contains large immature vesicles.

Later cleavages occur in vesicles after leaving the TGN, presumably due to activation of enzymes by the acidification of this granule (Orci et al., 1987; Anderson and Orci, 1988); these cleavages are blocked by monensin. We propose that the small amino terminal–containing vesicles that are transported to processes arise from the larger immature vesicles, although the evidence supporting this idea is not yet conclusive. In support of this idea, a higher proportion of processing intermediate immunoreactivity is found in the large vesicles (Kreiner et al., 1989). Furthermore, in [^{3}H]Phe-labeled experiments, a high concentration of autoradiographic grains is seen in mature small DCVs only after a 12-h chase but not at earlier time points (Table I). The large vesicles appear to have a short half-life since >50% of the counts associated with these vesicles appear in profiles that appear to be fated for degradation after a 12-h chase.

Mechanisms for Sorting Bag Cell Intermediates

The molecular mechanism by which the two processing intermediates are segregated from each other is still an open question. One appealing possibility is that the carboxy-terminal intermediate selectively condenses in the early region of the TGN, leaving the amino-terminal intermediate soluble. Perhaps different ionic conditions or different accessory proteins (Chung et al., 1989) located in the late region of the TGN would allow the amino-terminal portion of the prohormone to condense at this site. A differential timing of condensation has also been proposed to explain the separation of prolactin and growth hormone in somatomammotrophs (Fumagilli and Zanini, 1985). The aggregated carboxy-terminal portion of the precursor may be prevented from traveling to the late compartment either through steric hindrance of aggregates moving through small tubules, the inability to be packaged into small transport vesicles, or a specific association with an immobile membrane-bound receptor. Alternatively, movement of the amino-terminal portion of the precursor may be mediated through the actions of a membrane-bound recognition system. In support of this model, the bag cell amino-terminal intermediate (F2) is associated with membranes at a time point (30-min pulse and 2-h chase) when the carboxy-terminal intermediate (I3) is not membrane associated (Fisher, J., manuscript in preparation; illustrated in Fig. 8). A selective association of the amino-terminal intermediate with a membrane-bound receptor would allow a vesicular sorting mechanism similar to that proposed for lysosomal enzymes.

Implications of Bag Cell Neuron Sorting

The amino-terminal bag cell peptides act locally to modulate the electrical activity of abdominal ganglion neurons and in

an autocrine fashion to regulate the excitability of the bag cells (Rothman et al., 1983*a*; Kauer et al., 1987; Brown and Mayeri, 1989). The carboxy-terminal ELH acts both on nearby neurons (Mayeri et al., 1985) and through the circulation at peripheral targets as a hormonal substance (Kupfermann, 1967; Rothman et al., 1983*b*). Thus, while the polyprotein motif ensures cosynthesis, the relative levels of these two sets of substances are regulated by the proteolytic cleavage, packaging, and targeting described above. Recent studies indicate that non-ELH precursor-related bag cell vesicle proteins are also selectively sorted (Sossin and Scheller, 1989). These latter molecules may play a role in selective transport or release of different vesicle types. Other neurons that express the ELH prohormone (McAllister et al., 1983; Chiu and Strumwasser, 1984) may process and package the peptides differently than the bag cells, further illustrating ways in which the secretory pathway regulates intercellular communication.

We are very grateful to Dr. Michael Miller for providing us with his computer software to analyze the EM autoradiography and to Dr. Miller and Dave Saffitz for their assistance in using the software. Thane Kreiner introduced us to EM autoradiography. Fran Thomas provided excellent technical assistance. We thank William Trimble and Linda Ong for critical reading of the manuscript.

W. S. Sossin is supported by a studentship from the Medical Research Council of Canada. J. M. Fisher is part of the Medical Scientist Training program at Stanford University and is supported by a National Institutes of Health training grant. R.H. Scheller is a Presidential Young Investigator and a Pew scholar. This work is supported by a grant from the National Institute of Mental Health.

Received for publication 3 August 1989 and in revised form 26 September 1989.

References

Anderson, R. W. G., and L. Orci. 1988. A view of acidic intracellular compartments. *J. Cell Biol.* 106:539–543.

Berry, R., and S. Arch. 1981. Activation of neurosecretory cells enhances the synthesis of secretory protein. *Brain Res.* 215:115–123.

Brown, R. O., and E. Mayeri. 1989. Positive feedback by autoexcitatory neuroendocrine bag cells of *Aplysia*. *J. Neurosci.* 9:1443–1451.

Burgess, T. C., and R. B. Kelly. 1987. Constitutive and regulated secretion of proteins. *Annu. Rev. Cell Biol.* 4:243–293.

Campbell, C. H., and L. H. Rome. 1983. Coated vesicles from rat liver and calf brain contain lysosomal enzymes bound to mannose-6-phosphate receptors. *J. Biol. Chem.* 258:13347–13352.

Caro, L. G. 1969. A common source of difficulty in high resolution autoradiography. *Science (Wash. DC).* 41:918–920.

Caro, L. G., and R. P. Van Tubergen. 1962. High resolution autoradiography. *J. Cell Biol.* 15:173–177.

Chiu, A. Y., and F. Strumwasser. 1984. Two neuronal populations in the head ganglia of *Aplysia californica* with egg-laying hormone-like immunoreactivity. *Brain Res.* 294:83–93.

Chung, K. -N., P. Walter, G. W. Aponte, and H. -P. H. Moore. 1989. Molecular sorting in the secretory pathway. *Science (Wash. DC).* 243:192–197.

Crine, P., and L. Dufour. 1982. Effects of monensin on the processing of pro-opiomelanocortin in the intermediate lobe of the rat pituitary. *Biochem. Biophys. Res. Commun.* 109:500–506.

Davidson, H. W., C. J. Rhodes, and J. C. Hutton. 1988. Intraorganellar calcium and pH control proinsulin cleavage in the pancreatic B cell via two distinct site-specific endopeptidases. *Nature (Lond.).* 333:93–96.

Fisher, J. M., W. S. Sossin, R. Newcomb, and R. H. Scheller. 1988. Multiple neuropeptides derived from a common precursor are differentially packaged and transported. *Cell.* 54:813–822.

Friend, D. S., and M. J. Murray. 1965. Osmium impregnation of the Golgi apparatus. *Am. J. Anat.* 117:135–149.

Fumagalli, G., and A. Zanini. 1985. In cow anterior pituitary, growth hormone and prolactin can be packaged into separate granules in the same cell. *J. Cell Biol.* 100:2019–2024.

Gainer, H., Y. Sarne, and M. J. Brownstein. 1977. Neurophysin biosynthesis: conversion of a putative precursor during axonal transport. *Science (Wash. DC).* 195:1354–1356.

Griffiths, G., and K. Simons. 1986. The *trans*-Golgi network: sorting at the exit site of the Golgi complex. *Science (Wash. DC).* 234:438–443.

Griffiths, G., P. Qiunn, and G. Warren. 1983. Dissection of the Golgi complex. I. Monensin inhibits the transport of viral membrane proteins from *medial*- to *trans*-Golgi cisternae in baby hamster kidney cells infected with semliki forest virus. *J. Cell Biol.* 96:835–850.

Griffiths, G., B. Hoflack, K. Simons, I. Mellman, and S. Kornfeld. 1988. The mannose 6-phosphate receptor and the biogenesis of lysosomes. *Cell.* 52:329–341.

Hand, A. R., and C. Oliver. 1977. The role of the Golgi apparatus and GERL in secretory granule formation in acinar cells of the rat exorbital lacrimar gland. *J. Cell Biol.* 74:399–413.

Hashimoto, S., G. Fumagalli, A. Zanini, and J. Meldolesi. 1987. Sorting of three secretory proteins to distinct secretory granules in acidophilic cells of cow anterior pituitary. *J. Cell Biol.* 105:1579–1586.

Johnson, D. C., and M. J. Schlessinger. 1980. Vesicular stomatitis virus and Sindbis virus glycoproteins transport to the cell surface is inhibited by ionophores. *Virology.* 103:407–424.

Kauer, J. A., T. E. Fisher, and L. K. Kaczmarek. 1987. Alpha bag cell peptide directly modulates the excitability of the neurons that release it. *J. Neurosci.* 7:3623–3633.

Kelly, R. B. 1985. Pathways of protein secretion in eukaryotes. *Science (Wash. DC).* 230:25–32.

Kreiner, T., W. S. Sossin, and R. H. Scheller. 1986. Localization of *Aplysia* neurosecretory peptides to multiple populations of dense core vesicles. *J. Cell Biol.* 102:769–782.

Kreiner, T., J. M. Fisher, W. S. Sossin, and R. H. Scheller. 1989. Large dense cored vesicles are enriched in neuropeptide processing intermediates in the *Aplysia* bag cells. *Mol. Brain Res.* In press.

Kupfermann, I. 1967. Stimulation of egg laying: possible neuroendocrine function of bag cells of abdominal ganglia of *Aplysia californica*. *Nature (Lond.).* 216:814–815.

Loh, Y. P., M. J. Brownstein, and H. Gainer. 1984. Proteolysis in neuropeptide processing and other neural functions. *Annu. Rev. Neurosci.* 7:189–222.

Mayeri, E., B. S. Rothman, P. H. Brownell, W. D. Branton, and L. Padgett. 1985. Nonsynaptic characteristics of neurotransmission mediated by egg-laying hormone in the abdominal ganglion of *Aplysia*. *J. Neurosci.* 5:2060–2077.

McAllister, L. B., R. H. Scheller, E. R. Kandel, and R. Axel. 1983. *In situ* hybridization to study the origin and fate of identified neurons. *Science (Wash. DC).* 222:800–808.

Miller, M. I., K. B. Larson, J. B. Saffitz, D. J. Snyder, and L. J. Thomas, Jr. 1985. Maximum-likelihood estimation applied to electron microscopic autoradiography. *J. Electron Microsc. Tech.* 2:611–636.

Newcomb, R., and R. H. Scheller. 1987. Proteolytic processing of the *Aplysia* egg-laying hormone and R3-14 neuropeptide precursors. *J. Neurosci.* 7:854–863.

Newcomb, R., J. Fisher, and R. H. Scheller. 1988. Processing of the ELH precursor in the bag cell neurons of *Aplysia*. *J. Biol. Chem.* 263:12514–12521.

Novikoff, P. M., A. B. Novikoff, N. Quintana, and J. -J. Haun. 1971. Golgi apparatus, GERL, and lysosomes in neurons of rat dorsal root ganglia studied by thick section and thin section cytochemistry. *J. Cell Biol.* 50:859–886.

Orci, L., P. Halban, M. Amherdt, M. Ravazzola, J. D. Vassalli, and A. Perrelet. 1984. A clathrin-coated Golgi-related compartment of the insulin secreting cell accumulates proinsulin in the presence of monensin. *Cell.* 39:39–47.

Orci, L., M. Ravazzola, M. J. Storch, R. G. W. Anderson, J. D. Vassalli, and A. Perrelet. 1987. Proteolytic maturation of insulin is a post-Golgi event which occurs in acidifying clathrin-coated secretory vesicles. *Cell.* 49:865–868.

Orci, L., M. Ravazzola, M. Amherdt, A. Perrelet, S. K. Powell, D. L. Quinn, and H. -P. H. Moore. 1988. The transmost cisternae of the Golgi complex: a compartment for sorting of secretory and plasma membrane proteins. *Cell.* 51:1039–1051.

Pfeffer, S. R., and J. E. Rothman. 1987. Biosynthetic protein transport and sorting by the endoplasmic reticulum and Golgi. *Annu. Rev. Biochem.* 56:829–852.

Rothman, B. S., E. Mayeri, R. O. Brown, P. -M. Yuan, and J. E. Shively. 1983*a*. Primary structure and neuronal effects of alpha bag cell peptide, a second candidate neurotransmitter encoded by a single gene in bag cell neurons of *Aplysia*. *Proc. Natl. Acad. Sci. USA.* 80:5753–5757.

Rothman, B. S., G. Weir, and F. E. Dudek. 1983*b*. Egg-laying hormone: direct action on the ovotestis of *Aplysia*. *Gen. Comp. Endocrinol.* 52:134–141.

Saltpeter, M. M., and T. Bachmann. 1972. Autoradiography. *In* Principles and Techniques of Electron Micrography. Vol. 2. M. A. Hayat, editor. Van Nostren Reinholdt, New York. 221–276.

Saltpeter, M. M., and M. G. Farquhar. 1981. High resolution analysis of the secretory pathway in mammotrophs of the rat anterior pituitary. *J. Cell Biol.* 91:240–246.

Scheller, R. H., J. F. Jackson, L. B. McAllister, B. S. Rothman, E. Mayeri, and R. Axel. 1983. A single gene encodes multiple neuropeptides mediating a stereotyped behavior. *Cell.* 35:7–22.

Smith, R. E., and M. G. Farquhar. 1966. Lysosome function in the regulation of the secretory process in cells of the anterior pituitary gland. *J. Cell Biol.*

31:319–349.
Sossin, W. S., and R. H. Scheller. 1989. A bag cell neuron-specific antigen localizes to a subset of dense cored vesicles in *Aplysia californica*. *Brain Res.* 494:205–214.
Sossin, W. S., J. M. Fisher, and R. H. Scheller. 1989. Cellular and molecular biology of neuropeptide processing and packaging. *Neuron.* 2:1407–1417.
Tartakoff, A. M. 1983. Perturbation of vesicular traffic with the carboxylic ionophore monensin. *Cell.* 32:1026–1028.
Tooze, J., and S. A. Tooze. 1986. Clathrin-coated vesicular transport of secretory proteins during the formation of ACTH-containing secretory granules in AtT20 cells. *J. Cell Biol.* 103:839–850.
Tooze, J., M. Hollinshead, R. Frank, and B. Burke. 1987*a*. An antibody specific for an endoproteolytic cleavage site provides evidence that pro-opiomelanocorticotropin is packaged into secretory granules in AtT-20 cells before its cleavage. *J. Cell Biol.* 105:155–162.
Tooze, J., S. A. Tooze, and S. D. Fuller. 1987*b*. Sorting of progeny coronavirus from condensed secretory proteins at the exit from the *trans*-Golgi network of AtT20 cells. *J. Cell Biol.* 105:1215–1226.
von Figura, K., and A. Hasilik. 1986. Lysosomal enzymes and their receptors. *Annu. Rev. Biochem.* 55:167–195.
Williams, M. A. 1977. Preparation of EM autoradiographs. *In* Practical Methods in Electron Microscopy. A. M. Glauert, editor. Elsevier Science Publishers, B. V., Amsterdam. 77–155.
Yates, M. E., and R. W. Berry. 1984. Subcellular sites of processing of precursors of neurosecretory peptides in the bag cells of *Aplysia*: inferences from the effects of monensin, FCCP, and chloroquine. *J. Neurobiol.* 15:141–155.